Production of secondary neutrinos and photons in cosmic-ray sources environment

Denis Allard[*]

*Laboratoire Astroparticules et Cosmologie (APC), Université Paris 7/CNRS, 10 rue A. Domon et
L. Duquet, 75205 Paris Cedex 13, France.*
E-mail: denis.allard@apc.univ-paris7.fr

In this paper, we study the propagation of very high and ultrahigh energy cosmic-ray (VHE and
UHECRs) in their source environment and the production of secondary messengers (gamma-rays
and neutrinos). We primarily focus on the case of magnetized environments (galaxy clusters or
filaments) that are likely to surround a good fraction of UHECR sources. We discuss the escape
of primary cosmic-rays, the possible modifications of the injected composition triggered by the
source environment and the possibility to detect neutrino and gamma-ray signals produced by
cosmic-ray interactions. We finally briefly discuss the interest of the detection of gamma-ray and
neutrino signatures of the acceleration of UHECRs in the context of the latest results released by
the Pierre Auger Observatory.

1. Introduction

Despite several decades of experimental efforts, the origin of ultrahigh energy cosmic-rays (UHECRs) remains a mystery. Recent experiments (primarily the Pierre Auger Observatory[1]) have allowed a very significant increase of the statistics above 10^{18} eV and high resolution measurements of the UHECR spectrum, composition and arrival directions. The current data are, however, not sufficient to shed a complete light on the UHECRs origin and statistics at the highest energies (around and above 10^{20} eV) is still sorely missing due to the flux suppression observed by both HiRes[2] and Auger[3] above 3-5$\times 10^{19}$ eV. Moreover, some controversies (and possibly inconsistencies) remain between the results released by the different experiments especially from the point of view of the UHECR composition and arrival directions. One of the possible way to improve our understanding of the UHECR phenomenon is to improve the current experimental capabilities by building larger aperture detectors, such as JEM-EUSO[4], that should provide a much larger statistics above $5\,10^{19}$ eV. On the other hand, very important complementary informations could be brought by looking for multi messenger (gamma-rays and neutrinos) signatures of the acceleration or the propagation of UHECRs.

In this paper we consider the production of secondary photons and neutrinos during the propagation of VHE and UHE cosmic-rays in the magnetized environment of the sources. We consider two particular cases. First, a UHECR source in the environment of a galaxy cluster. In this case, we take into account the radial evolution of the magnetic field and the intra-cluster enhancement of the photon and baryon densities. We discuss the impact of this environment on the escape of UHECRs protons and nuclei and the production of secondary gamma-rays and neutrinos. Second, we consider the case of a UHECR source within a magnetized filament and study the possibility of detecting the synchrotron signature (see below) of the propagation of freshly accelerated UHECRs (as previously suggested by [5]) in this environment. Finally, we discuss the potential interest and "added value" of the detection of these UHECR acceleration multimessenger signatures to solve the puzzle of UHECRs origin, we place this discussion in the context of the latest results from the Pierre Auger Observatory.

2. Secondary neutrinos and photons from galaxy clusters environment

2.1 Modeling of the intra-cluster environment

In this section, we study the propagation of VHE and UHE protons and nuclei in a galaxy cluster environment[1]. Our modeling of the galaxy clusters and its environment for either cool core and non cool core cluster is using the output of 3D MHD from [7]. The cool core cluster, we selected has the following properties: $R_{200} = 1.1\,h^{-1}$Mpc (the radius below which the matter overdensity exceeds a factor of 200), the virial mass $M_{200} \equiv 200 \times (4\pi/3)\rho_c R_{200}^3 = 3.5 \times 10^{14}\,h^{-1}M_\odot$ (where ρ_c is the critical density), and the X-ray temperature $T_X = 5.1$keV. The radial profile of the magnetic field intensity and turbulence scale as well as the baryon density and the location and mass of the galaxies are directly given by the simulations. The radial profile of the magnetic field intensity

---

[1]A full presentation of the details of the modeling and the results of this study can be found in [6] and references therein
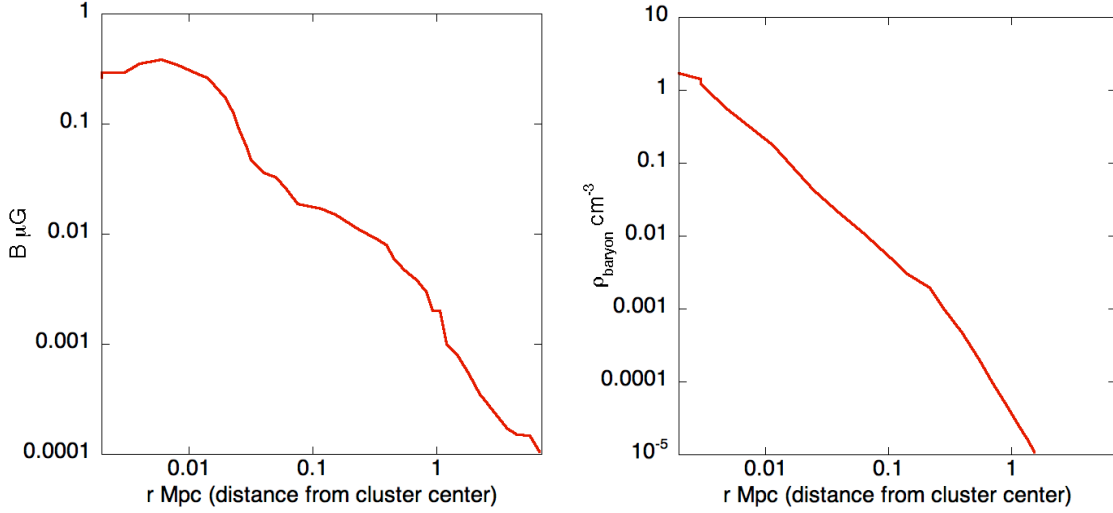
Figure 1: Left: Magnetic field intensity radial profiles for a cool core cluster from the simulations of [7]. Right: Baryonic density radial profiles averaged in azimuth from the same structure simulations.

and the baryon density for a cool core cluster are given in Fig. 1. In our calculations, we use the magnetic field radial profile given by the simulations and leave the normalization at the center as a free parameter varying from 1 to 30 μG. The turbulent field coherence length varies from ~ 20 kpc in the central regions to ~ 150 kpc for R $\geq$ R$_{200}$. We use the fast trajectory integration method from [8] to compute cosmic-ray trajectories through the intracluster turbulent magnetic fields. Another necessary ingredient in order to estimate cosmic-ray energy losses during their propagation in the cluster environment is the modeling of the intra-cluster photon background. For that purpose we assume that the galaxies inside the cluster are elliptical and have a typical spectral energy distribution (SED) equivalent to the estimate of [9] for this type of galaxies. With the photon and baryon density profile we are able to compute the interaction rate of protons and nuclei as a function of their energy and location in the cluster. For photo interactions of we use the monte-carlo code described in [10] that includes a treatment of the proton photopion interactions using the SOPHIA [11] event generator. In addition, the hadronic interactions are treated (assuming the intracluster baryons are protons) using the EPOS 1.6 model[12]. The mean free path for the different interaction mechanisms of protons and nuclei (photon induced and hadronic interactions) are displayed in Fig. 2

2.2 propagation and escape of VHE and UHECR protons and nuclei

We first study the propagation and escape of protons and nuclei from the cluster environment. During their journey within the cluster, charged cosmic-ray can be confined by the large ambient magnetic fields and interact with enhanced photons and baryon backgrounds. In particular, galaxy clusters can be a hostile environment for heavy nuclei that are expected to be more efficiently confined at a given energy and should suffer more from energy looses due to their larger interaction cross sections (see Fig.2). As a case study, we placed a source (most likely an AGN) at the center of the cluster, located at 100 Mpc from the earth, assuming a mixed composition similar to that of low
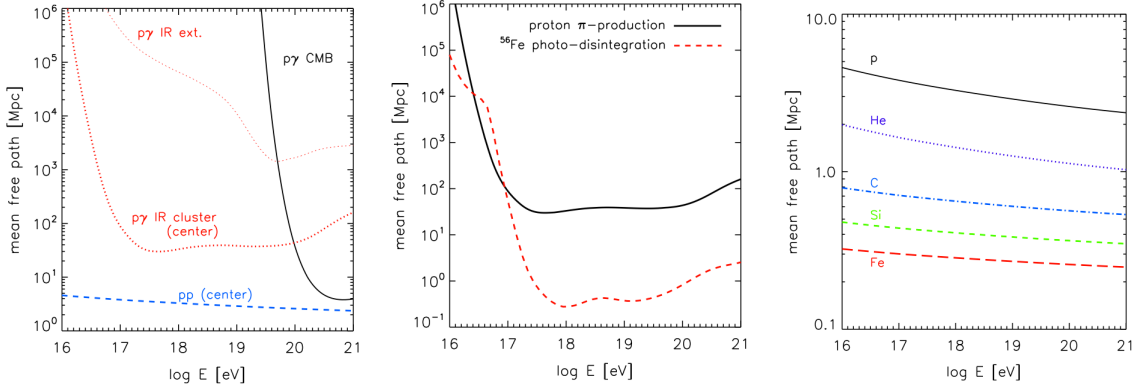
Figure 2: Left: Energy evolution of protons mean free path in the central region a a cool core cluster. The contributions of hadronic (pp) interaction (dashed blue lines), photopion interactions with the intracluster photon background (thick red dotted line), extragalactic infra-red photon background [13] (thin red dotted line) and CMB (black line) are shown. Center : Comparison of the proton photopion (black line) and iron photodisintegration (red dashed line) mean free paths with the intracluster photon background at the center of the cluster. Right panel: Hadronic interaction (Np) mean free paths for proton, helium, carbon, silicon, and iron nuclei according to the EPOS 1.6 interaction model, the density of ambient protons is set to $1\,\mathrm{cm}^{-3}$

energy galactic cosmic-ray, a spectral index $\beta = 2.3$ (see [14]) and a luminosity $L_{cr} = 10^{45}\,\mathrm{erg\,s}^{-1}$ (L_{cr} is defined as the cosmic-ray luminosity between 1 GeV and $E_{max} = Z \times 10^{20.5}\,\mathrm{eV}$, for a spectral index 2.3, it is close to the luminosity required to produce the whole UHECR spectrum with a source density $n_s = 10^{-5}\,\mathrm{Mpc}^{-3}$). We propagate cosmic-rays above 10^{16} eV until they leave the cluster (i.e, they reach a distance larger than 5 Mpc from the cluster center) or their energy falls below 10^{15} eV. Fig. 3a shows the resulting (i.e, escaping from the cluster environment) cosmic-ray spectrum for the cool core cluster of galaxies for a magnetic field normalization at 3μG at the center. The flux is decomposed between different elemental groups (see labels). One can observe features in the spectra of the different nuclei, which increase in amplitude with the mass of the nuclei and the normalization of the magnetic field. At the lowest energies, the flux of the heaviest nuclei is greatly suppressed due to hadronic interactions. In the same energy range, light and intermediate nuclei suffer less interactions due to their larger mean free paths ($\lambda \propto A^{-2/3}$) and rigidities (as the confinement time $\tau_{conf} \propto (E/Z)^{-1/3}$). As the baryonic density rapidly decreases with the distance to the center and the confinement time with the energy, hadronic interactions become less efficient to disintegrate nuclei above $E \sim 10^{17}$ eV. Above this energy, however, heavy nuclei start to interact with optical and near-infrared photons. For lighter nuclei, the energy threshold for photo-interactions is lower (more or less proportional to the mass of the nuclei A) but the mean free path is larger (more or less proportional to A^{-1}); therefore, photodisintegration has a lower impact. Above $E \sim A \times 4 \times 10^{18}$ eV, nuclei are completely disintegrated by Cosmic Microwave Background (CMB) photons and turn into secondary nucleons of energy A times lower. Let us note that these interactions (unlike those at lower energies) are not due to the cluster environment, as nuclei are barely confined by the cluster magnetic field at these energies; they would take place in a similar way in the intergalactic medium. Unlike complex nuclei, the proton component is soften at low energy due to the addition of secondary nucleons resulting from nuclei interactions and then shows

4
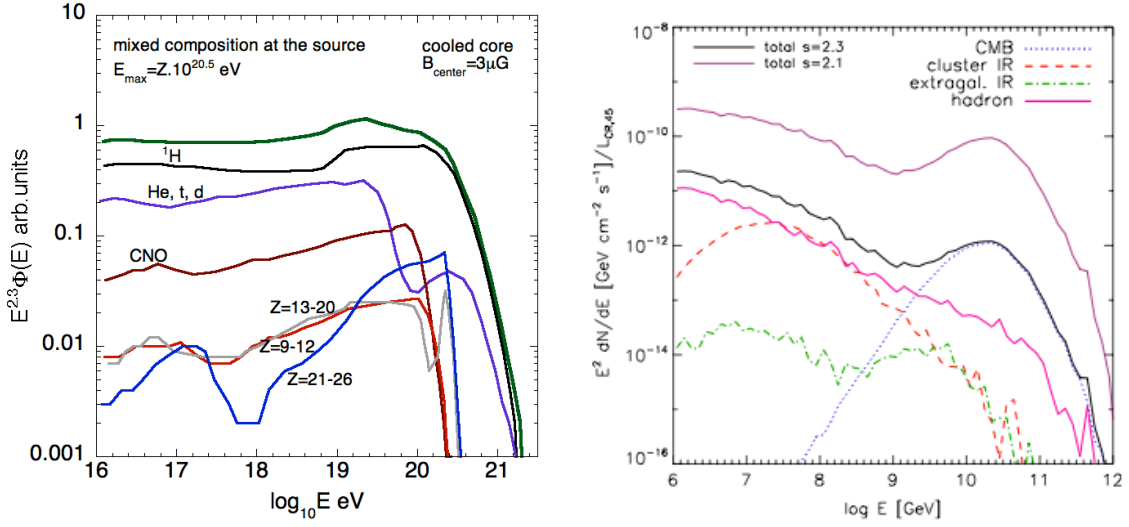
Figure 3: Left: Cosmic-ray spectrum escaping from the cluster environment assuming a central source emitting a mixed composition (see text), the contribution of different elemental groups is shown. Right: Corresponding neutrino emission, the contribution of the different interaction processes is shown (see label), the case of a source with same luminosity above 1 GeV but a spectral index β=2.1 is also displayed.

a bump above 4×10^{18} eV due to disintegration of nuclei by CMB photons. The amplitude of the above described features depend on the normalization of the field can be significantly increased for central fields above 10 μG. On the other end, due to the sharp radial profile of the field intensity, a slight offset of the source from the cluster center would decrease the confinement time in the cluster environment as well as the interaction rate[2]. Let us note that we assumed, in the previous calculations, that a stationary regime was reached. It might not be the case for typical AGN lifetimes for the values of the magnetic field we assumed, the essential features of the non stationary regime are discussed in [6]. In any case, this case study shows that such a magnetized environment together with enhanced baryon and photon backgrounds can strongly modify the accelerated cosmic-ray output in the vicinity of the source.

2.3 Neutrino production

One of the main interest of such a magnetized and dense environment is to enhanced the production of secondary neutrinos and photons. These secondaries are produced by hadronic and photo-induced interactions. In the case of complex nuclei, secondaries are mostly provided by hadronic interactions of the primary fragments and photo-interactions of the secondary nucleons. The secondary neutrino flux associated with the above described source and the contribution of the different interaction channels are displayed in Fig. 3b. Above 1 PeV, the neutrino spectrum is quite steep and dominated by hadronic interactions which are especially efficient at low energy due to the increase of the confinement time in the central regions while above $\sim 10^{18}$ eV interactions with CMB photons start to dominate. Although, the enhancement of the expected neutrino flux is quite large at PeV energies, it is still well below experiment capabilities as far as point sources are con-

---

[2]It would also decrease the production of secondary photons and neutrinos we discuss in the following.

cerned. The case a source with the same cosmic-ray luminosity above 1 GeV but a spectral index 2.1 (i,e, a source $\sim$ 25 (resp. 60) times more powerful above 10^{16} (resp. 10^{18}) eV is also shown. For such a source luminosity (that should be quite unusual in the local universe ($\sim 10^{-7}\,\mathrm{Mpc}^{-3}$) not to overshoot the UHECR spectrum), the PeV neutrino flux is an order of magnitude larger but still below $10^{-9}\,\mathrm{GeV\,cm^{-2}\,s^{-1}}$ and a luminosity one order of magnitude larger would be needed for such a point-like (or slightly extended) source to be detected by current or planned experiments like Ice-Cube or Km3Net. Detection at PeV energies would however not be a signature of UHECR acceleration as these neutrinos are mostly produced by cosmic-rays primaries below 10^{18} eV. Although, we showed that the detection at PeV energies of such a neutrino source requires very large cosmic-ray luminosities (that would involve sources that are very rare in local universe), these luminosities are much lower than those required from the propagation in the intergalactic medium[3] (see [15, 16]).

2.4 Gamma-ray production

The same interaction processes as well as pair creation are expected to produce VHE and UHE photons and e^+e^- pairs. Unlike neutrinos these particles are expected to cascade down to GeV-TeV energies in the cluster environment and in the intergalactic medium. Synchrotron emission is moreover expected to efficiently cool e^+e^- pairs due to the large magnetic fields in the cluster. The photon fluxes produced in the cluster and expected on earth are displayed in Fig. 4a. One can see that most of the gamma-ray flux arriving on earth is produced inside the cluster with a large contribution of the synchrotron mechanism below $\sim$100 GeV. For the source luminosity assumed in the previous paragraphs ($L_{cr} = 10^{45}\,\mathrm{erg\,s^{-1}}$ above 1 GeV and β=2.3), the expected photon fluxes (that are more over expected to have an angular extension at least as large as that of the cluster) are pretty low. The contribution of lower energy cosmic-rays (below 10^{16} eV) is however missing in Fig.4a. The contribution of low energy cosmic-rays is, indeed expected to be important as the production of VHE photons and pair inside the cluster is dominated by hadronic interactions. Low energy cosmic-ray have a similar interaction rate (due to the flat energy evolution of the cross-section) but a much larger confinement time in the central region than high energy particles. We calculated their contribution with an analytical method, the result is displayed in Fig. 4b. The photon flux produced inside the cluster and expected on earth are much larger due to this additional contribution. The fluxes displayed even overshoot some known limits from cluster observations by EGRET and the total diffuse flux would obviously overshoot the observed ones (see [6] for more details). The GeV-TeV expected flux can however be lowered if one assumed a harder source spectral index that would lead to a lower fraction of the luminosity given to low energy cosmic-ray or if the minimum energy of cosmic-rays released by the source is much higher than 1 GeV as illustrated in Fig. 4c. In any case, the cascade photon from hadronic interactions within galaxy cluster environment can certainly easily be spotted by future gamma-ray experiment such as CTA providing the angular size of the signal remains low enough. Those gamma-ray should be more easily detectable than the previously mentioned PeV neutrinos. The latter are however potentially bringing additional

---

[3]PeV cosmogenic (i,e, from the propagation in the intergalactic medium) are, moreover, unlikely to correlate with their source due to the magnetic deflexion expected during the propagation of cosmic-rays on very large distances.
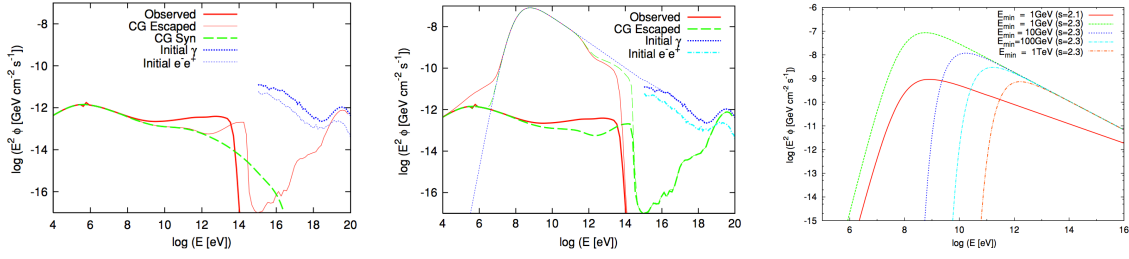
Figure 4: Left: Gamma-ray emission assuming the same conditions as in Fig. 3. Blue dotted lines represent electron and positron (thin) and photon (thick) fluxes produced in the cluster by cosmic rays above 10^{16} eV. Green dashed lines indicate the contribution of synchrotron emission inside the cluster. The red thin line is the gamma-ray flux obtained after propagation in the cluster of galaxies, that one would observe at a distance of 100 Mpc in absence of electromagnetic cascades in the intergalactic medium. The thick red line indicates the photon flux observed at 100 Mpc after cascading in the intergalactic medium. Center: Same as left panel (see labels), with the additional contribution of cosmic-rays between 1 GeV and 10^{16} eV. Right: gamma-ray fluxes produced by low-energy cosmic rays ($E \leq 10^{16}$ eV) assuming spectral indices of 2.1 (red solid) and 2.3, with different minimum injection energy E_{min} = 1, 10, 100, and 10^3 GeV. For the case of a 2.1 spectral index the source luminosity above 1 GeV is assumed to be $L_{cr} = 2 \times 10^{43}\, erg\, s^{-1}$.

constraints, the gamma-ray signal being simply a signature a cosmic-ray acceleration in the central region without giving a clear clue about the presence of trans-PeV or trans-EeV cosmic-rays.

3. Synchroton signatures of UHECR acceleration in magnetized filaments

3.1 Principle of the calculations

Besides galaxy clusters, filamentary structures of matter are also expected to harbor non negligible magnetic fields. In this section, we study the production and detectability of gamma-ray signatures of the acceleration of UHECRs from a source located in the center of an extragalactic filament (see [18] for more details and further references). Although, the matter density and magnetic fields are supposed to be lower in filaments than in galaxy clusters, these probably magnetized regions are promising for the detection of gamma-ray signal. Indeed, once UHECRs have escape from their source (where they may or may not suffer interactions), they propagate through the extragalactic medium. At the highest energies, particles are likely to experience photopion interactions (and to a lower extend pair production) in the vicinity of the source. Most of the energy losses result in the emission of e$^+$e$^-$ pairs (disintegration of charged pions or pair production) and photons that can interact and produce pairs. In a magnetized environment these pairs can produce directly GeV-TeV synchrotron gamma-rays instead of further cascading creating gamma-ray halos with spatial and angular extension similar to that of the magnetized structure. We study this possibility first introduced by [5] in the case of magnetic filaments. As in the case of galaxy clusters, the filamentary structure we use in our simulations is extracted from large scale structure formation simulations. We assume the average value of the magnetic field in the intergalactic medium to be of the order of 1 nG and use different hypotheses on the scaling of the magnetic field with matter density (see [18] for more details). We use the code described in the previous section but in the

case of filaments we do not consider any enhancement of the photon and baryon backgrounds in the source environment, in other words we assume hadronic interactions to be negligible.[4]

3.2 Results

The gamma-ray spectra we obtain, assuming that a source located in the center of the filament with luminosity $L_{cr} = 10^{42} \, erg \, s^{-1}$ above 10^{19} eV (which is more or less equivalent to $L_{cr} = 10^{45} \, erg \, s^{-1}$ above 1 GeV for a 2.3 spectral index considered in the previous section) is observed along the axis of the filament (there is a weak dependence on the line of sight orientation discussed in [18]), is displayed in Fig. 5a. For our choice for the field normalization, the emission is peaked around 10 GeV with fluxes approaching $10^{-12} \, GeV \, cm^{-2} \, s^{-1}$. The peak is mostly produced by pairs created by photopion interctions which means that such a signal signal is a signature of the presence of particles accelerated above 10^{20} eV. On the other hand, these fluxes are well below the point source sensitivities of Fermi in the GeV range and CTA around one TeV. For a source located at 100 Mpc a luminosity ∼100 times larger would be required (i.e, $L_{cr} = 10^{44} \, erg \, s^{-1}$ above 10^{19} eV) for the gamma-rays to be observed. The angular profiles of the gamma-ray emission that would be observed on earth for a source located at 100 Mpc[5] ($L_{cr} = 10^{44} \, erg \, s^{-1}$) and 1 Gpc ($L_{cr} = 10^{46} \, erg \, s^{-1}$) integrated between 1 and 100 GeV are displayed in the central panel of Fig. 5. The source at 1 Gpc has the advantage of keeping a smaller angular extension that would make its detection by CTA around 1 TeV easier. Moreover, with the luminosity needed to allow the possibility of a detection by Fermi or CTA, the source located at 100 Mpc would practically overshoot the UHECR spectrum by itself whereas the source located at 1 Gpc keeps a much lower contribution due to UHECR energy losses (see discussion in [18, 16]). As a conclusion, the synchrotron signatures of the acceleration of UHECR above 10^{20} eV (or more exactly above the pion production threshold) are quite promising probes of the UHECRs origins, they are however most likely to be detectable for extremely powerful (hence, rare and distant) sources. Let us note that although this synchrotron signal is expected to be lower than the total cascade signal, the latter is highly likely to suffer from isotropization and dilution if the extragalactic magnetic fields in the void is of the order or larger than 1 pG (see discussion in [19]).

4. Discussion and conclusion

Let us note that the neutrino signal around 10^{18} eV for a source with similar luminosity as considered in the previous section (i.e, $L_{cr} = 10^{46} \, erg \, s^{-1}$ above 10^{19} eV at 1 Gpc) would reach $\sim 10^{-9} \, GeV \, cm^{-2} \, s^{-1}$, i.e, a level that might be reachable by Ice Cube or Km3Net depending on their sensitivities at very high energy (see [16]). At first sight, the very large luminosity required for the detection of clear signatures of the acceleration of UHECR at the highest energies is not particularly encouraging. It is however important to place this discussion in the context of the recent composition analysis published by the Pierre Auger collaboration [20]. The Pierre Auger Observatory recently reported the largest statistics composition studies above 10^{19} eV based on the

---

[4]This is a necessary condition for the signal we study in this section not to be overwhelmed by the one produced by low energy cosmic-rays.

[5]As these luminosities above 10^{19} eV are very large we consider spectral indexes β=2.0 to avoid prohibitive energy budgets when extrapolating back to low energies.
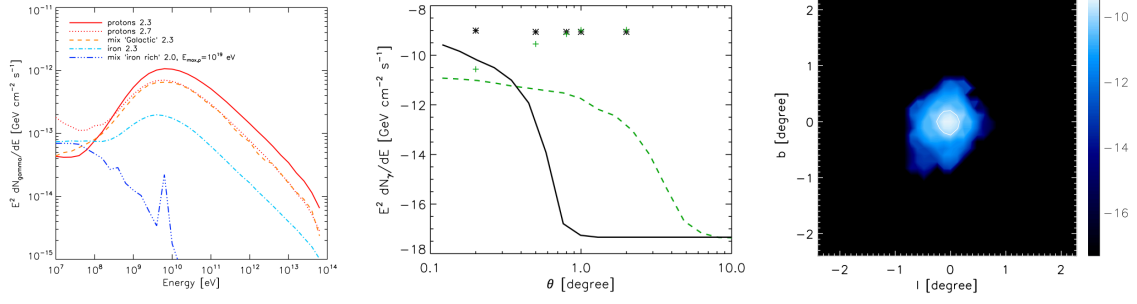
Figure 5: Left: Photon flux produced by synchrotron emission for different source compositions and injection spectral indexes. The source has a luminosity of $L_{cr} = 10^{42}\,erg\,s^{-1}$ and is located in a filament at a distance of 100 Mpc. Center: Angular profiles of the gamma-ray flux integrated over energies $E_\gamma = 1$?100 GeV for a filament seen along its axis, at 1 Gpc and $L_{cr} = 10^{46}\,erg\,s^{-1}$ (black solid line), and at 100 Mpc and $L_{cr} = 10^{44}\,erg\,s^{-1}$ (green dashed line). The black stars and green crosses present the corresponding integrated flux up to a given angular extension. Right: Gamma-ray image corresponding to the angular profile of the source located at 1 Gpc on the central panel. (note that further cascading of gamma-rays above a few TeVs is not considered)

energy evolution of the maximum of longitudinal development of air shower (X_{max}) and its spread. The X_{max} energy evolution behaves as if the composition was gradually becoming heavier with energy, from a light composition around the ankle to a much heavier composition above a few 10^{19} eV. Such an evolution of the composition is difficult to justify above 10^{19} eV if all the different species present in the source composition are accelerated to the highest energies (above 10^{20} eV), in which case the composition should get lighter. The most likely explanation of the observed trend involves models where the maximum energy per unit charge is limited around $Z \times 10^{19}$ eV or below, *i.e.* models assuming that the proton component is not accelerated at the highest energies unlike heavy nuclei (see [21]).

However, one could argue that a dispersion of the maximum energy at the sources is possible (if not likely). Using the famous Hillas criterion one can show that (for the simplest derivations) magnetic luminosities above $10^{45}\,erg\,s^{-1}$ (see [22, 23] are required to accelerate protons above 10^{20} eV whereas this condition is much looser for heavy nuclei[6]. The composition trend suggested by Auger might then be due the fact that sources able to accelerate protons at the highest energies are extremely rare in the "GZK horizon" and are outnumbered by weaker sources that can reach energies around 10^{20} eV only for heavy nuclei. In this context gamma-ray and neutrino observatories might bring an opportunity to observe UHECR protons acceleration signatures from distant and very luminous sources (i.e, far outside the cosmic-ray horizon above 10^{19} eV). In the current context of a UHECR composition dominated by nuclei at the highest energies, these potential observations would be a very important piece of information for our understanding of UHECRs origin.

---

[6]these simple considerations do not include energy losses in the acceleration site besides expansion or synchrotron losses.

References

[1] Abraham et al. [Pierre Auger Collaboration], 2004, Nuclear Instruments and Methods in Physics Research Section A, vol. 523 pp. 50.

[2] Sokolsky P. and Thomson G. B., 2007, Journal of Physics G: Nuclear and Particle Physics vol. 34, pp. 401.

[3] Abraham et al. [Pierre Auger Collaboration], 2008, Phys. Rev. Let. vol. 101, pp. 61101.

[4] Medina-Tanco G. et al. [JEM-EUSO collaboration], 2009, arXiv:0909.3766.

[5] Gabici S. and Aharonian F., 2005, Phys. Rev. Let., vol. 95 pp. 251102.

[6] Kotera K., Allard D., Murase K., Aoi J. , Dubois Y., Pierog T., Nagataki S., 2009, ApJ, vol. 707 pp. 370.

[7] Dubois Y. and Teyssier R. 2008, A&A, 482, L13.

[8] Kotera K. and Lemoine M., 2008, Phys. Rev. D. vol. 77, pp. 23005, arXiv:0706.1891.

[9] Lagache G., Puget J.-L. and Dole H. 2005, ARA&A, 43, 727.

[10] Allard D. and Protheroe R. J., 2009, A&A, vol. 502 pp. 803.

[11] Mucke A., Engel R., Rachen J. P., Protheroe R. J., and Stanev T. 2000, Comp. Phys. Com., 124, 290.

[12] Werner K., Liu F.-M. and Pierog T., 2006, Phys. Rev. C, 74, 044902

[13] Stecker F. W., Malkan M. A. and Scully S. T., 2006, ApJ 648, 774Ð783.

[14] Allard D., Parizot E., Khan E., Goriely S. and Olinto A. V., 2005, A&A Letters, 443, 29, astro-ph/0505566.

[15] Essey W., Kalashev O. E., Kusenko A. and Beacom J. F., 2010, Phys. Rev. Let., vol. 104 pp. 141102.

[16] Decerprit G. and Allard D., 2011, A&A in press, arXiv:.

[17] Murase K., 2009, Phys. Rev. Lett., 103, 081102.

[18] Kotera K., Allard D. and Lemoine M., 2011, A&A, vol. 527 pp. 54.

[19] Gabici S. and Aharonian F., 2007, Astrophysics and Space Science, vol. 309 pp. 465.

[20] Abraham et al. [Pierre Auger Collaboration], 2010, Phys. Rev. Let., vol. 104 pp. 91101.

[21] Allard D., Busca N. G., Decerprit G., Olinto A. V. and Parizot E., 2008, Journal of Cosmology and Astro-Particle Physics 10, 33.

[22] Achterberg A., 2002, proceedings of les Houches summer school, Accretion disks, jets and high energy phenomena in astrophysics.

[23] Lemoine M. and Waxman E., 2009, Journal of Cosmology and Astroparticle Physics, vol. 11 pp. 009.